This article has been accepted for publication in a future issue of this journal, but has not been fully edited. Content may change prior to final publication. Citation information: DOI 10.1109/TIA.2018.2808905, IEEE Transactions on Industry Applications

Integrated Topology of DC-DC Converter for LED Street Lighting System Based on Modular Drivers

Cassio Gobbato, Samuel Valerio Kohler, Ithalo Hespanhol de Souza, Gustavo Weber Denardin and Juliano de Pelegrini Lopes
Federal University of Technology - Paraná (UTFPR)
Pato Branco, Paraná, Brazil
cassiogobbato@gmail.com

***Abstract*— This work proposes a LED luminaire for street lighting based on modular drivers. Each module consists of a driver composed by two integrated DC-DC converters. The first one is a buck-boost converter, responsible for the power factor correction, and the second is a buck converter, which controls the load current. Both of the converters operate in the discontinuous conduction mode of current. In order to make the system robust against failure, each driver supplies an independent set of power LEDs. Thus, in case of failure of one or more drivers, the system is not completely compromised. The design of the electronic drivers is presented. Experimental results of a prototype with rated power of 50 W (two modules of 25 W) are performed in order to show the feasibility of the proposed solution.**

***Index Terms*— DC-DC converters, light emitting diodes, modular drivers, power electronics, street lighting.**

I. INTRODUCTION

DUE to the incentive to reduce the electric energy consumption in the various classes of consumers, all forms of improve the energy efficiency of the electric and electronic equipment are important. In street lighting, the lamps based on light-emitting diodes (LEDs) technology [1]-[6] have been shown to be more efficient compared to the tradition high-pressure sodium (HPS) lamps, despite the still dominant use of HPS worldwide [7]. The power LEDs have reached luminous efficacy and lifetime higher than 200 lm/W and 60000 hours, respectively [8]. Moreover, the LEDs technology has no mercury in its composition. Therefore, the use of LEDs for street lighting lamps has proved to be a good alternative to save electric energy and it has been the goal of many researches [9]-[12].

The LED lamps are supplied by a circuitry known as driver, which must be able to process the electric energy from the line and supply the LEDs with a continuous current. The driver lifespan must be compatible with the LEDs so that the lamp does not lose one of its main features, the high lifetime [7], [9]. The main responsible for the low reliability of the drivers is the electrolytic capacitor, widely used in power electronics topologies. Such capacitor technology is responsible for about 50% of failures in switching power supplies [13]-[15], as well as presents a lifetime lower than the LEDs. The useful life of electrolytic capacitors is reduced by half if the operating temperature is increased by 10°C. Thus, with the natural heating of the LEDs, the lifetime of the electrolytic capacitor becomes the critical factor that determines the lifetime of the driver [16]. In order to improve the driver reliability, several works in the literature suggest the replacement of the electrolytic capacitors by film or polyester ones [16]-[19].

A LED driver is usually composed by two stages: Power Factor Correction (PFC) and Power Control (PC). Both of the stages are implemented by DC-DC converters. The converter used for PFC is responsible for the high power factor and meeting the IEC 61000-3-2 Class C standard regarding the current harmonics inject into the public supply system. The PC stage is responsible for the LED current control in order to provide a continuous current with a small ripple. Both PFC and PC stages have independent controlled switches and its command circuits, which increases the driver components number. Thus, some works have presented an alternative that integrates the PFC and PC stages, sharing the same controlled switch and its command circuit [19]-[21]. Therefore, the number of active switches and their command circuits are reduced, as well as the control complexity, but the switch voltage and/or current stresses are increased. Besides a common node, the integrated converters must operate at the same switching frequency and duty cycle.

Although the drivers used in street lighting have a high lifespan, they may present failures caused by manufacturing defect, inclement weather and oscillations in the line voltage, for example. On public places such as squares, streets, amusement parks and others, the lack of lighting can cause accidents and decrease safety until the damaged lamp be replaced, which may take weeks. Thus, this work proposes a LED luminaire for street lighting based on modular drivers. The design of modular drivers for street lighting based on LED lamps provides a more reliable system that keeps the lamp luminous flux, even that lower than the nominal one, in case of failure of one or more modules. It is important because it prevents unlit areas until system maintenance. In addition, a LED lamp composed by modules allows a simple design, which is independent of the lamp power. For example, for modules of 25 W it is possible to build a lamp with a rated power multiple of 25 W, by using a parallel association of “n” modules. It would be a good alternative for the manufacturers, making it possible to standardize the LED lamps driver design. Additionally, when one of the lamp drivers fails, just with the

This article has been accepted for publication in a future issue of this journal, but has not been fully edited. Content may change prior to final publication. Citation information: DOI 10.1109/TIA.2018.2808905, IEEE Transactions on Industry Applications

replacement of the damaged driver it is possible to obtain a lamp with its rated power again, while in the traditional not modular lamps all the driver is lost.

This paper is organized as it follows. In Section II the advantages of the LED modular driver luminaire are presented. Section III exposes the important points of the converters design. In Section IV the converters modeling and control design are shown. Sections V presents the experimental results and the discussions about it. Section VI presents an overview about the proposed topology and Section VII shows the conclusions of the paper.

II. Proposed Topology

In the modular proposed topology, the modules are connected in parallel and operate individually as shown in Fig. 1. Also, such modules have an individual LED current control. The controller is implemented by a microcontroller that is able to control any number of modules, depending only of the processing capacity and A/D converters speed. Fig. 2 shows the proposed circuitry of one lamp module. A buck-boost converter operating in the discontinuous conduction mode of current (DCM) was chosen for implement the PFC stage in this work. Such converter has been used in many papers for active PFC stage due to its desirable features [22]-[26]. For the PC stage, a buck converter is used also in DCM, being chosen because the output voltage is lower than the bus voltage in this work. Besides that, the buck converter has features that are interesting for LED lamps driver and it has been used in several works for this purpose [27]-[31].

III. Converters design

In this Section the main equations of the built prototype are shown. In Section III-A is presented the analysis of the PFC converter. Section III-B presents the PC converter analysis and the LED electrical model.

A. Power Factor Correction Converter

The design of the PFC converter is realized considering the equivalent circuit presented in [32], which is valid for any DC-

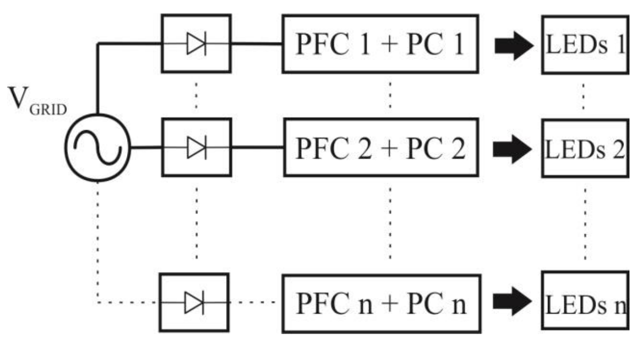

Fig. 1. Luminaire structure with "n" LED modular drivers.

DC converter operating in DCM. In this mode the converter emulates an electric resistance for the line. Thus, a high-power factor and a low input current Total Harmonic Distortion (THD) are obtained without a current closed-loop. The buck-boost inductor (L_{pfc}) is given by (1) [18].

$$L_{pfc} = \frac{V_{pk}^{2} \cdot D_{pfc}^{2} \cdot \eta_{pfc}}{4 \cdot f_s \cdot P_{bus}} \tag{1}$$

where V_{pk} is the peak value of the line voltage, D_{pfc} is the buck-boost duty cycle, η_{pfc} is the buck-boost efficiency, f_s is the switching frequency and P_{bus} is the buck-boost output power.

The bus capacitor (C_{bus}) is designed based on its stored energy and ripple requirements. It is calculated by (2) [2].

$$C_{bus} = \frac{V_{pk}^{2} \cdot D_{pfc}^{2}}{4 \cdot L_{pfc} \cdot f_s \cdot V_{bus} \cdot \omega_r \cdot \Delta V_{bus}} \tag{2}$$

where ω_r is the line voltage frequency, V_{bus} is the bus voltage and ΔV_{bus} is the bus voltage ripple. Through (1) and (2) it is observed that, by decreasing P_{bus}, the L_{pfc} increases and C_{bus} decreases. Thus, another advantage of building a modular LED lamp is the reduction of the bus capacitor, which makes possible to use a polyester or a film capacitor.

B. Power Control Converter

The main function of the PC converter is to compensate the bus voltage low-frequency ripple and regulates the load average current. So, the PC design parameters have to consider the critical operating condition for it stage, which is the minimum bus voltage. Thus, PC converter inductance (L_{pc}) is obtained by (3).

$$L_{pc} = \frac{\left[\left(\frac{2 \cdot D_{pc} \cdot \eta_{pc} \cdot V_{bus\min}}{V_{out}} - D_{pc}\right)^{2} - D_{pc}^{2}\right] \cdot V_{out}}{8 \cdot f_s \cdot I_{leds}} \tag{3}$$

where D_{pc} is the buck converter duty cycle, η_{pc} is its efficiency, V_{out} and I_{leds} are the PC converter output voltage and current, respectively.

The output capacitor (C_{out}) is responsible by filtering the high-frequency voltage ripple and it is given by (4).

$$C_{out} = \frac{\left(V_{bus\min} - V_{out}\right) \cdot D_{pc}}{16 \cdot L_{pc} \cdot \Delta V_{out} \cdot f_s^{2}} \tag{4}$$

where ΔV_{out} is the buck converter output voltage ripple.

This article has been accepted for publication in a future issue of this journal, but has not been fully edited. Content may change prior to final publication. Citation information: DOI 10.1109/TIA.2018.2808905, IEEE Transactions on Industry Applications

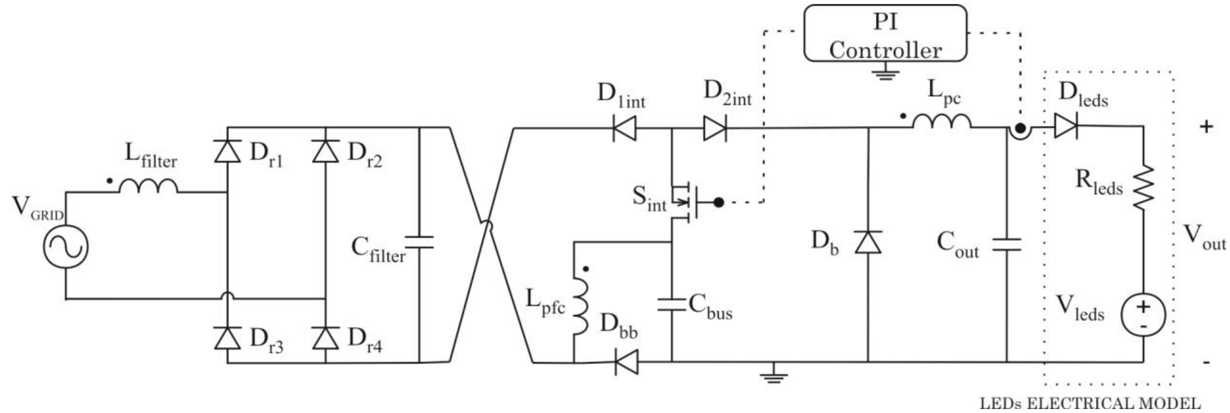

Fig. 2. Schematic of one module with the integrated buck-boost and buck converters.

C. LED Electrical Model

The LED electrical model is presented in Fig. 3 and consists of an ideal diode (D_m), a resistor (R_m) and a voltage source (V_m) that represents the minimum voltage required for the LED be forward biased.

In this work 15 LEDs (model P3-D-White by Wayjun Technology Co., Ltd) are in series connection for each module. By a linear regression of the current per voltage characteristic curve of the LED were obtained 2.84V and 0.76Ω for V_m and R_m, respectively.

D. Integrated Topology

As mentioned above, two DC-DC converters can be integrated if both circuits share a common node and operate at the same switching frequency and duty cycle [22].

If the buck-boost and buck converters shown in Fig. 4a and Fig. 4b are in series connection, the drains of the switches share the same node. This configuration is known as T-type inverted [22]. Thus, the integration is performed replacing the S_{bb} and S_b switches by S_{int} switch and adding two diodes D_{1int} and D_{2int} as shown in Fig. 2. The duty cycle of the integrated switch must attend both the PFC and PC critical duty cycle, given by (5) and (6), respectively.

$$D_{bbc} \leq \frac{V_{bus}}{V_{pk}+V_{bus}} \tag{5}$$

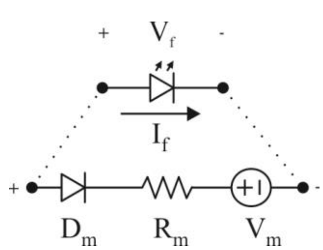

Fig. 3. LED electrical model.

$$D_{bc} \leq \frac{V_{out}}{V_{bus}} \tag{6}$$

The design parameters and main components of each modular driver are presented in Table I and Table II, respectively.

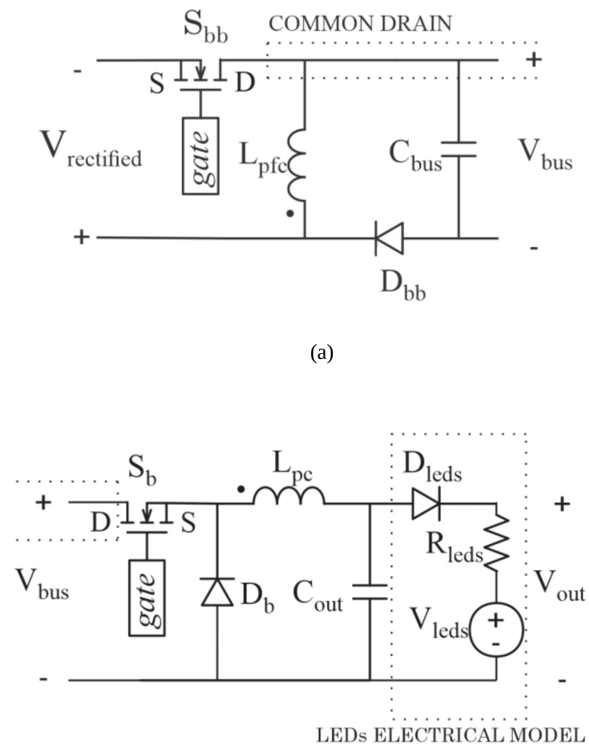

(a)

(b)

Fig. 4. Integrated topology with common drain: (a) Inverted buck-boost converter. (b) Buck converter.

This article has been accepted for publication in a future issue of this journal, but has not been fully edited. Content may change prior to final publication. Citation information: DOI 10.1109/TIA.2018.2808905, IEEE Transactions on Industry Applications

TABLE I
DESIGN PARAMETERS

SYMBOL	SPECIFICATION	VALUE
V_{GRID}	Mains voltage (RMS)	127V
f_r	Mains frequency	60Hz
P_o	Output power (each module)	25W
I_{leds}	Output current (average)	500mA
V_{bus}	PFC output voltage (average)	170V
V_{out}	PC output voltage (average)	51V
η_{pfc}	PFC converter efficiency	95%
η_{pc}	PC converter efficiency	90%
ΔI_{leds}	LEDs current ripple	100mA - 20%
ΔV_{bus}	PFC output voltage ripple	85V - 50%
ΔV_{out}	PC output voltage ripple	1.02V - 2%
f_s	Switching frequency	60 kHz

TABLE II
DESIGNED COMPONENTS

SYMBOL	SPECIFICATION	VALUE
D_{r1}-D_{r4}	Diode UF4007	700V / 1A
$L_{filter1}$	Thornton EE-30/15/7	3.198mH / $R_{filter1}$=10.8Ω
$L_{filter2}$	Thornton EE-30/15/7	3.188mH / $R_{filter2}$=11.5Ω
C_{filter}	Polyester capacitor	330nF / 250V
D_{bb}	Diode UF5408	1000V / 3A
D_b	Diode UF5408	1000V / 3A
L_{pfc1}	Thornton E30/15/7	590.4μH / R_{Lpfc1}=2.21Ω
L_{pfc2}	Thornton E30/15/7	576.3μH / R_{Lpfc2}=2.04Ω
C_{bus}	Polyester capacitor	4.7μF / 250V
S_{int}	Switch IRF840	500V / 8A $R_{ds(on)}$=0.85Ω
D_{int1}	Diode UF5408	1000V / 3A
D_{int2}	Diode UF5408	1000V / 3A
L_{pc1}	Thornton E30/15/7	346.8μH / R_{Lpc1}=1.07Ω
L_{pc2}	Thornton E30/15/7	332,4μH / R_{Lpc2}=0,95Ω
C_{out}	Polyester Capacitor	2.2μF / 250V
$LEDs$	P3-D-White	3.2V / 700mA

IV. PC CONTROLLER DESIGN

As stated in the previous section, the proposed converter relies in high PFC bus voltage ripple and reduced output power per module to allow the use of a polyester or film capacitor. However, such approach also increases the current at the switch and the LED current ripple, if it is applied an open loop power converter [33]. Depending on the range of the current ripple, the LED functionality can be compromised. Therefore, a controller should be used in order to maintain the average LED current as close as possible to the design parameters and to reduce the low frequency ripple in the LED current [7]. Several controller techniques can be employed to achieve this goal. As it is intended to obtain a low computation time for the controller, a proportional-integral (PI) controller is proposed to obtain zero steady-state error. It is crucial to remember that one microcontroller can be used to control several power modules, which is the reason to use a controller with reduced complexity.

In (7) is presented the transfer function of a PI controller.

$$C(s) = K_P \frac{\left(s + \frac{K_I}{K_P} \right)}{s} \tag{7}$$

where K_P and K_I are the proportional and integral gains of the PI controller.

To a proper PI design, the controller parameters should be specified based on the errors that is intended to mitigate or, if possible, eliminate. Consequently, to start such analyses, it is necessary to model the dynamics of all components of the power and control circuitry (power converters, filters, etc.).

Although the power system stages are integrated, each converter operates individually. In other words, the PFC converter is a voltage source for the buck converter and, the buck converter is the load of the PFC converter, which due to the DCM operation mode behaves as an equivalent resistance. Thus, one can simplify the PFC stage output as a constant voltage source and, simply model the power control stage.

The transfer function that should be used for designing the LED current control is the one that relates the duty cycle of the buck converter with its output current. Such function is obtained resolving the equivalent circuit given by the Averaged Switch Model (ASM), which relies on averaging the waveforms over one switching cycle to remove the switching frequency and its harmonics [34]. Fig. 5 shows the simplified buck converter DC averaged model.

Note that R_e is the buck converter equivalent resistance shown in (8), and $P_{inb}(t)$ represents the power consumed by R_e.

$$R_e = \frac{2 \cdot L_{pc} \cdot f_S}{D_{pc}{}^2} \tag{8}$$

It is important to observe that the circuit shown in Fig. 5 is non-linear. Thus, it is necessary to construct a small-signal equivalent circuit model, wherein the signals of the averaged model are perturbed about a quiescent operating point, as shown in (9)-(13).

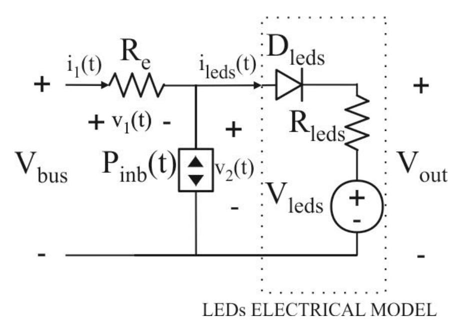

Fig. 5. Buck converter (DCM) DC averaged model.

This article has been accepted for publication in a future issue of this journal, but has not been fully edited. Content may change prior to final publication. Citation information: DOI 10.1109/TIA.2018.2808905, IEEE Transactions on Industry Applications

$$d_b(t) = D_{pc} + \hat{d}_{pc}(t) \tag{9}$$

$$\langle v_1(t) \rangle = V_1 + \hat{v}_1(t) \tag{10}$$

$$\langle i_1(t) \rangle = I_1 + \hat{i}_1(t) \tag{11}$$

$$\langle v_2(t) \rangle = V_2 + \hat{v}_2(t) \tag{12}$$

$$\langle i_{leds}(t) \rangle = I_{leds} + \hat{i}_{leds}(t) \tag{13}$$

where D_{pc}, V_1, I_1, V_2 and I_{leds} are the quiescent values of the averaged signals applied to the model and $\hat{d}_{pc}$, $\hat{v}_1$, $\hat{\imath}_1$, $\hat{v}_2$ and $\hat{\imath}_{leds}$ are small variations about the respective quiescent values.

In [34] this analysis is presented, in which the linearization is accomplished using the Taylor expansion about the operation point and retaining only the constant and linear terms. Based on such approach it is possible to obtain a transfer function that relates the LEDs current with duty cycle, as shown in (14) [34].

$$G_{i_{leds}}(s) = \frac{\dfrac{V_{bus}\left(V_{bus} - V_{out}\right) D_{pc} T_s}{2 V_{out} L_{pc} C_{out} R_{leds}}}{s + \left(\dfrac{1}{R_{leds} C_{out}} + \dfrac{{V_{bus}}^2 {D_{pc}}^2 T_s}{2 L_{pc} {V_{out}}^2 C_{out}} \right)} \tag{14}$$

where T_S is the switching period.

The selected operating point for the controller design is the minimum bus voltage, which causes the PC converter to operate with its maximum duty cycle. Fig. 6 shows the system block diagram. Note that in addition to the PI controller and the plant transfer function, the block diagram presents a $H_{A/D,CS}$ function block at the feedback line. Such function represents the Hall Effect sensor that is used to provide the current feedback.

Fig. 7 presents the feedback diagram. The ACS712 Hall Effect sensor produces a voltage proportional to the input current. This sensor has a first order low-pass filter with the user-defined cut-off frequency. By reducing the bandwidth of the sensor output, it is possible to improve the current resolution, due to the reduction of the peak-to-peak noise. However, despite its advantages in the sensor current resolution, a drastic reduction in the sensor bandwidth jeopardizes the controller performance. Thus, based on the switching frequency and closed-loop analysis, such filter is tuned to 20 kHz by a 4.7nF capacitor and the 1.7kΩ internal resistor. Finally, a FRDM-KL25Z microcontroller kit implement the discrete PI controller, using a 12 bits A/D converter and an ARM cortex-M0 processor.

As previously mentioned, in the proposed system each power module has its own PI controller. In such controller an integrator is applied to eliminate steady state errors. Furthermore, one can note from the system transfer function that the current control loop is stable with only one single dominant pole. In these cases, a straightforward method is to allocate the zero of the PI controller to cancel the dominant pole of the plant. Such approach is known as pole placement. After that a 2nd order closed-loop system is obtained, which makes possible to conclude the controller design by parameters as rising time and damping ratio, which are directly related to the system bandwidth. Moreover, in the used methodology such design parameters may be specified as a function of the controller gains.

Finally, by applying the PI controller in the PC stage, K_P and K_I gains will determine how fast the controller can compensate the low frequency ripple at 120 Hz. However, high gains could cause two side effects. The first one to verify is the system stability, which due to the pole placement approach is the simplest to solve, by limiting the gain based on the required rising time and overshoot. The second one is related to the input current THD. In a PFC converter in

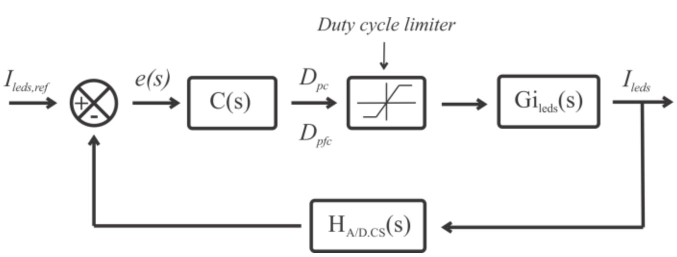

Fig. 6. PC Control loop using PI controller.

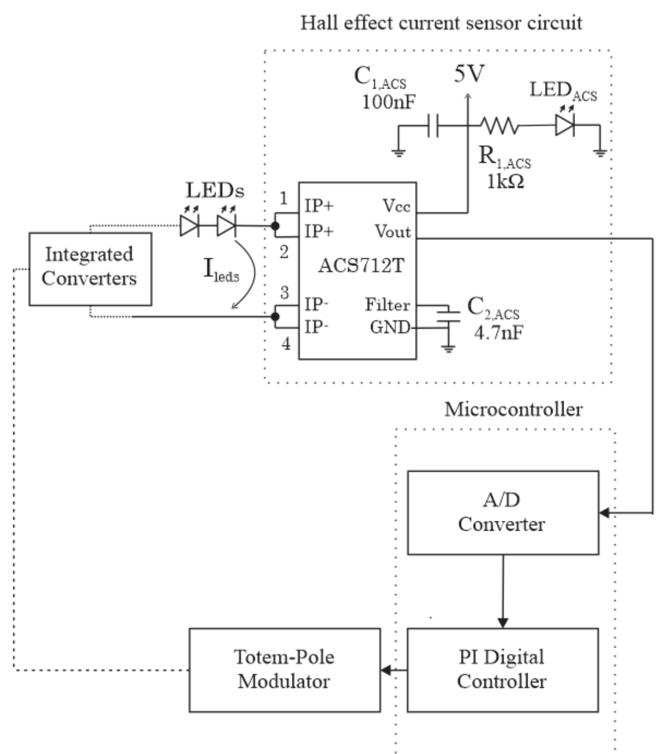

Fig. 7. Feedback diagram.

This article has been accepted for publication in a future issue of this journal, but has not been fully edited. Content may change prior to final publication. Citation information: DOI 10.1109/TIA.2018.2808905, IEEE Transactions on Industry Applications

discontinuous conduction mode and at constant duty cycle, the input current tracks the sinusoidal shape of the input voltage. Nevertheless, the PFC and PC stages are integrated in the proposed system, which implies in a variable duty cycle of the PFC converter if the PI controller changes the PC duty cycle. Such variation has the effect to modify the PFC current tracking property, which could lead the input current to a higher THD and, possibly, lose its compliance with the IEC 61000-3-2 standard. Therefore, considering these two possible side effects, the controller is tuned as shown in (15).

$$C(s)=\frac{(1+2.7\cdot 10^{-5}\cdot s)}{s}\cdot 19541 \tag{15}$$

The obtained closed-loop system is stable based on the gain and phase margin criteria. Hence, one should verify the controller performance, which is possible by the analysis of the step response for the compensated system, as shown in Fig. 8. Note that the closed-loop system response is similar to the open loop, but without the steady-state error. Despite a better controller performance is limited by the two factors previously discussed, it can be seen that there is no system overshoot and the rising time is fast enough to compensate the 120 Hz ripple.

V. Experimental Results

In order to evaluate the proposed luminaire based on modular drivers, it was developed a prototype consisting of two modules, as shown in Fig. 9. Note that in this circuit only one microcontroller is used to control the two modules.

Fig. 10 and Fig. 11 show the waveforms of the input current, voltage and power at 127 V_{rms} mains voltage for the modules 1 and 2, respectively. Based on the sum of the input power of both modules, the average input power of the proposed luminaire is 61.3W.

The measured value of each current harmonic is obtained from the Tektronix DPO3054 oscilloscope, configured to the IEC 61000-3-2 Class C Standard. In Fig. 12 it is possible to verify that all input current harmonics are in compliance with the IEC 61000-3-2. Additionally, the obtained total harmonic distortion is 14.7% and the real power factor is 0.957.

Fig. 13 shows the bus voltage in both modules. The average value of the voltage is 166 V (V_{bus1}) and 150 V (V_{bus2}) in the modules 1 and 2, respectively. One can verify that both bus voltages are lower than the designed value. This occurs because the converters are integrated and operate in closed-loop. So, when the duty cycle is modified, the bus voltage is also modified.

The output power, current and voltage of the both modules are presented in Fig. 14 and Fig. 15.

It is possible to note that the measured output current is close to the nominal one, wherein such difference from the design value is due to the current sensor resolution. In the used sensor there is a compromise between the bandwidth and current resolution, which limits the closed-loop performance. This also impacts the total average output power, which is slightly higher than the design value, being 52.61 W for both modules. Thus, the measured luminaire efficiency is 85.82%. One can note that similar efficiency should be obtained with more than two modules, which enables obtaining luminaires of higher output power (75W, 100W, etc.) without reducing efficiency.

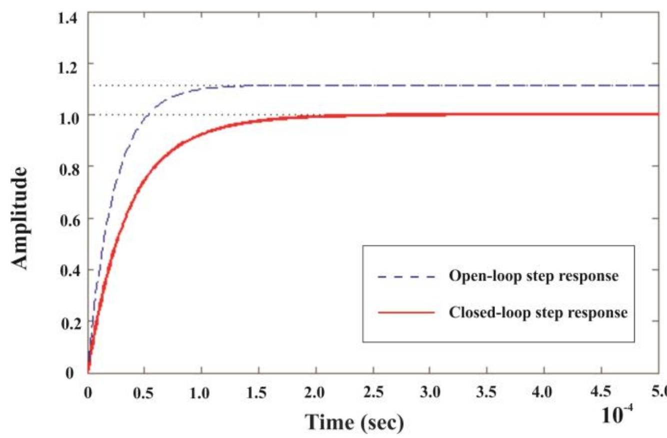

Fig. 8. Step response of the open-loop plant and the compensated system.

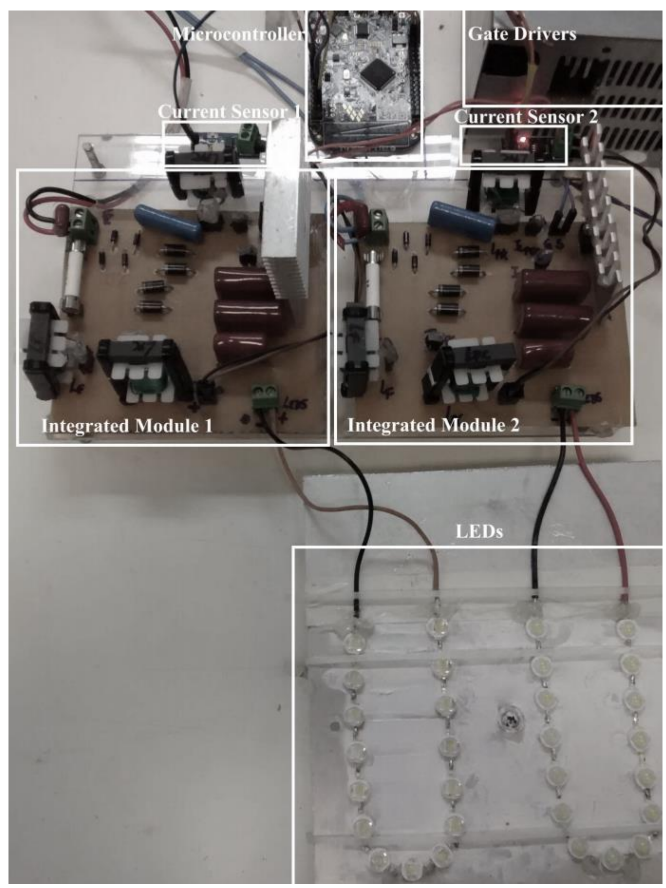

Fig. 9. Laboratory prototype of the proposed luminaire.

This article has been accepted for publication in a future issue of this journal, but has not been fully edited. Content may change prior to final publication. Citation information: DOI 10.1109/TIA.2018.2808905, IEEE Transactions on Industry Applications

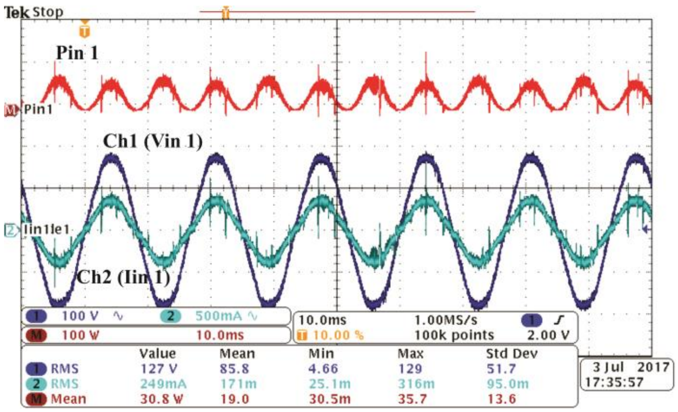

Fig. 10. Module 1: line voltage and current at nominal power and 127 Vrms line voltage. (100 V/div, 500 mA/div, 100 W/div, 10 ms/div).

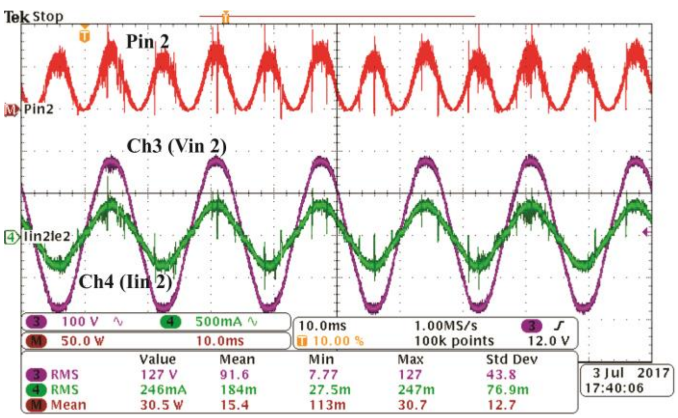

Fig. 11. Module 2: line voltage and current at nominal power and 127 Vrms line voltage. (100 V/div, 500 mA/div, 50 W/div, 10 ms/div).

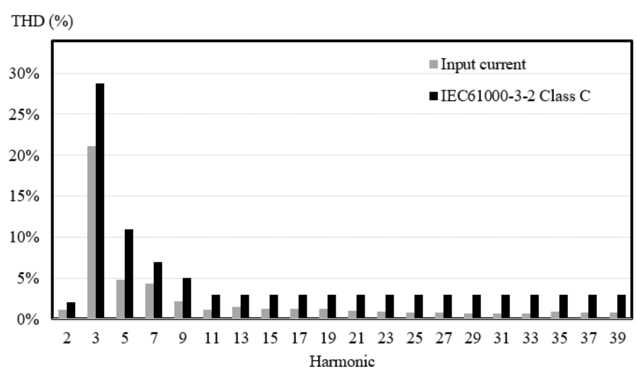

Fig. 12. Input current spectrum in comparison with IEC61000-3-2 Standard.

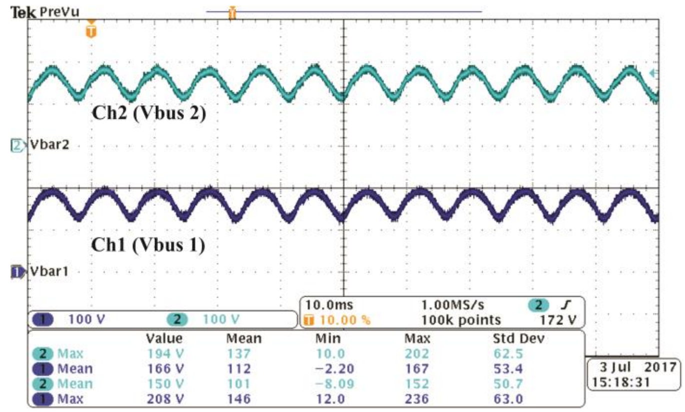

Fig. 13. Bus voltage in both modules. (100 V/div, 10 ms/div).

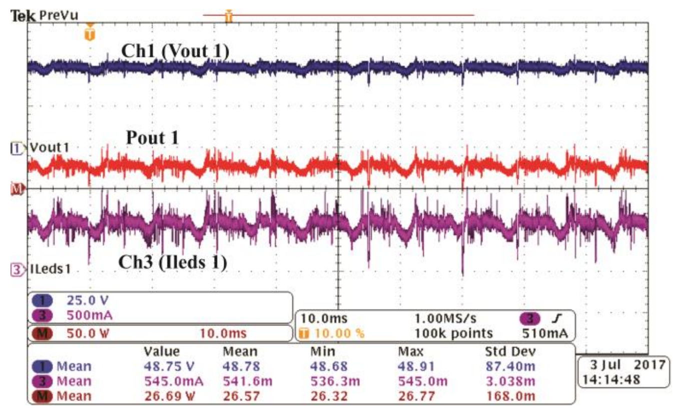

Fig. 14. Output power of the module 1. (50 W/div, 25 V/div, 500 mA/div, 10 ms/div).

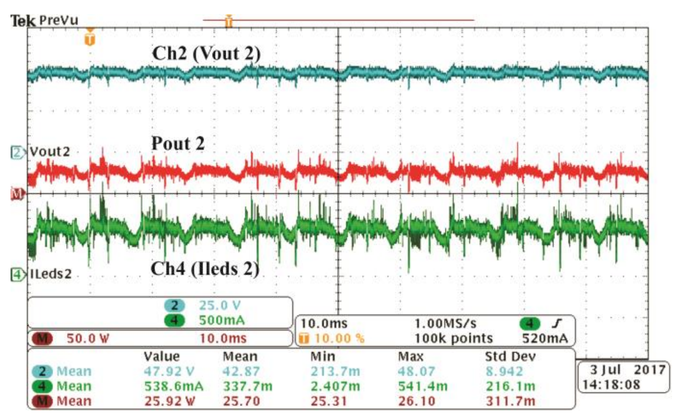

Fig. 15. Output power of the module 2. (50 W/div, 25 V/div, 500 mA/div, 10 ms/div).

VI. Discussion

In this section it is intended to clarify some of the choices embraced in the proposed topology. At first, the use of a two-stage converter topology made it possible to reduce the bus capacitor value. Consequently, this allowed the choice for non-electrolytic capacitors, which helps to increase the useful life of the system [35]. In addition, the processing of lower power (25 W) favors the use of non-isolated or integrated converters, which reduces the LED driver size, cost and complexity [36], [37]. In [38] a modular topology with a single input and several outputs is presented. This implies a higher power processing in the PFC stage (300 W, in such case), which reflected in larger passive components, for instance, the PFC bus capacitor. Such approach may reduce the system reliability, as a failure in the PFC stage will compromise the entire system. Hence, the use of low power PFC integrated to the power converter proposed in this paper does not suffer this drawback.

Assuming the previous stated advantages of using multi-stage converters, the integration of the stages presents

This article has been accepted for publication in a future issue of this journal, but has not been fully edited. Content may change prior to final publication. Citation information: DOI 10.1109/TIA.2018.2808905, IEEE Transactions on Industry Applications

conditions that favor the use in modular topologies, such as smaller average cost than multiple independent stages, lower control complexity and reduction of the command circuitry. However, the integration of stages also increases the voltage and current stress in the semiconductors. For example, by integrating two stages, one single controlled switch is shared with the converters. This switch must be designed so that to support the sum of the voltages or currents of each transistor before the integration, depending on the connection point. Considering the case of voltages sum, it is required a transistor with a higher voltage rating, which is usually followed by a larger on resistance. These factors, added to a high voltage and current stress scenario, will increase the switch power losses [35]. Thus, the operating power of each module should not be high, in order to maintain the advantages of the modular integrated converters. Therefore, an investigation was carried out to verify the efficiency of the proposed topology as a function of the processed power by theoretical analysis and simulations. The obtained results are presented in Fig. 16.

It can be seen from Fig. 16 that the overall efficiency decreases with the increase of the processed power. Thus, considering the proposed modular topology for street lighting, converters of 25 W offers a suitable compromise between cost and efficiency. In addition, such power value allows to implement the most common rated power of street lighting fixtures, according to the specified association (50 W, 75 W, 100W, etc.).

Such analysis complies with the literature and can be supported by the obtained results in related works. In [39], [40] integrated topologies with higher power are presented. Prototypes of 70 W and 100 W presented an efficiency of 84% and 80.6% respectively. However, it should be noted that the efficiency of LED drivers also depends on the design characteristics of each prototype, such as: number of stages, converter topology, used components and closed-loop control.

For all these reasons, it is recommended to use low power integrated converters in a modular topology, preferably not exceeding 50 W.

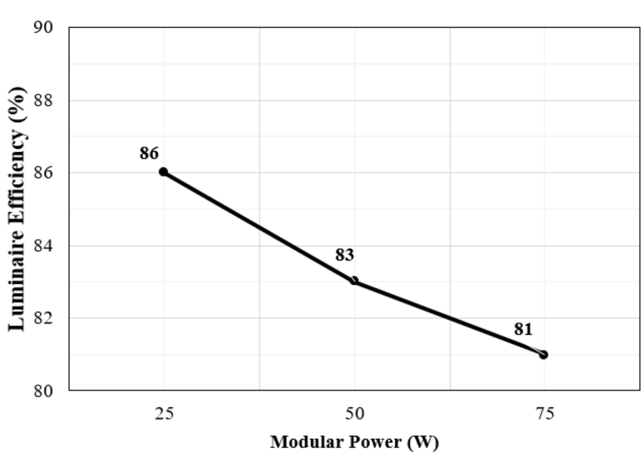

Fig. 16. Proposed topology efficiency as a function of the processed power.

VII. Conclusion

In this paper a topology for street lighting systems based on LED modular drivers has been presented. A luminaire composed by modules avoids the total failure of the lamp, maintaining its operation with a lower power than the nominal one until the system maintenance. A prototype of 50 W was designed, implemented, tested and the presented experimental results were satisfactory. The bus capacitance value was decreased by increasing the ripple at the bus voltage around 50% and due to the reduced power of each module, which allowed the use of a non-electrolytic capacitor. In order to limit the LED current ripple, a digital PI controller was implemented.

The proposed modular street lighting lamp, which relies on low power modules, allows to maintain the main features of the lamp as close as possible to the characteristics of one individual module, regardless of the total lamp power, for instance, efficiency and absence of electrolytic capacitor. It makes the proposed solution suitable for efficient street lighting systems based on LED lamps.

Acknowledgment

The authors gratefully acknowledge the support for this work provided by CAPES, CNPq, Fundação Araucária and FINEP.

References

[1] L. Lohaus, A. Rossius, S. Dietrich, R. Wunderlich and S. Heinen, "A Dimmable LED Driver With Resistive DAC Feedback Control for Adaptive Voltage Regulation," in *IEEE Transactions on Industry Applications*, vol. 51, no. 4, pp. 3254-3262, July-Aug. 2015.

[2] R. A. Pinto, J. M. Alonso, M. S. Perdigão, M. F. da Silva and R. N. do Prado, "A New Technique to Equalize Branch Currents in Multiarray LED Lamps Based on Variable Inductors," in *IEEE Transactions on Industry Applications*, vol. 52, no. 1, pp. 521-530, Jan.-Feb. 2016.

[3] M. F. de Melo, W. D. Vizzotto, P. J. Quintana, A. L. Kirsten, M. A. Dalla Costa and J. Garcia, "Bidirectional Grid-Tie Flyback Converter Applied to Distributed Power Generation and Street Lighting Integrated System," in *IEEE Transactions on Industry Applications*, vol. 51, no. 6, pp. 4709-4717, Nov.-Dec. 2015.

[4] M. Cole, H. Clayton and K. Martin, "Solid-State Lighting: The New Normal in Lighting," in *IEEE Transactions on Industry Applications*, vol. 51, no. 1, pp. 109-119, Jan.-Feb. 2015.

[5] D. Gacio, J. M. Alonso, J. Garcia, D. Garcia-Llera and J. Cardesín, "Study on Passive Self-Equalization of Parallel-Connected LED Strings," in *IEEE Transactions on Industry Applications*, vol. 51, no. 3, pp. 2536-2543, May-June 2015.

[6] D. Jenkins and A. Bhargava, "LED Lighting: Maximizing the Reliability, Safety, and Efficiency of Light Fixtures in Hazardous Environments," in *IEEE Industry Applications Magazine*, vol. 21, no. 1, pp. 64-67, Jan.-Feb. 2015.

[7] D. Camponogara, D. R. Vargas, M. A. Dalla Costa, J. M. Alonso, J. Garcia and T. Marchesan, "Capacitance reduction with a converter connection applied to LEDs." *IEEE Trans. Ind. Electron.*, vol. 62, no. 1, pp. 184–192, Jan. 2015.

[8] Osram, "OSRAM Opto Semiconductors", Internet: www.osram.com/os/ [June 21, 2017].

[9] C. A. Cheng, C. H. Chang, T. Y. Chung and F. L. Yang, "Design and Implementation of a Single-Stage Driver for Supplying an LED Street-Lighting Module With Power Factor Corrections," in *IEEE Transactions on Power Electronics*, vol. 30, no. 2, pp. 956-966, Feb. 2015.

[10] C. A. Cheng, H. L. Cheng and T. Y. Chung, "A Novel Single-Stage High-Power-Factor LED Street-Lighting Driver With Coupled Inductors," in *IEEE Transactions on Industry Applications*, vol. 50, no. 5, pp. 3037-3045, Sept.-Oct. 2014.

[11] H. Jin, S. Jin, L. Chen, S. Cen and K. Yuan, "Research on the Lighting Performance of LED Street Lights With Different Color Temperatures," in *IEEE Photonics Journal*, vol. 7, no. 6, pp. 1-9, Dec. 2015.

[12] Y. Wang, Y. Guan, K. Ren, W. Wang and D. Xu, "A Single-Stage LED Driver Based on BCM Boost Circuit and LLC Converter for Street Lighting System," in *IEEE Transactions on Industrial Electronics*, vol. 62, no. 9, pp. 5446-5457, Sept. 2015.

[13] D. Lamar, M. Arias, A. Rodriguez, A. Fernandez, M. M. Hernando and J. Sebastian, "Design-oriented analysis and performance evaluation of a low-cost high-brightness LED driver based on flyback power fator corrector," *IEEE Trans. Ind. Electron.*, vol. 60, no. 7, pp. 2614–2626, Jul. 2013.

[14] R. Pinto, M. Cosetin, A. Campos, M. Dalla Costa, and R. do Prado, "Compact emergency lamp using power LEDs," *IEEE Trans. Ind. Electron.*, vol. 59, no. 4, pp. 1728–1738, Apr. 2012.

[15] B. Wang, X. Ruan, K. Yao, and M. Xu, "A method of reducing the peakto-average ratio of LED current for electrolytic capacitor-less AC/DC drivers," *IEEE Trans. Power Electron.*, vol. 25, no. 3, pp. 592–601, Mar. 2010.

[16] Y. Qin, H.-H. Chung, D. Lin, and S. Hui, "Current source ballast for high power lighting emitting diodes without electrolytic capacitor," *34th IEEE IECON*, 2008, pp. 1968–1973.

[17] B. Sun, X. Fan, L. Li, H. Ye, W. van Driel and G. Zhang, "A Reliability Prediction for Integrated LED Lamp With Electrolytic Capacitor-Free Driver," in *IEEE Transactions on Components, Packaging and Manufacturing Technology*, vol. 7, no. 7, pp. 1081-1088, July 2017.

[18] H. S.-H. Chung, N.-M. Ho, W. Yan, P. W. Tam, and S. Y. Hui, "Comparison of dimmable electromagnetic and electronic ballast systems an assessment on energy efficiency and lifetime," *IEEE Trans. Ind. Electron.*, vol. 54, no. 6, pp. 3145–3154, Dec. 2007.

[19] C. Gobbato, S. V. Kohler, I. H. de Souza, G. W. Denardin and J. de Pelegrini Lopes, "Integrated topology of DC converter for street lighting system based on LED modular drivers," *2016 12th IEEE International Conference on Industry Applications (INDUSCON)*, Curitiba, 2016, pp. 1-6.

[20] P. C. V. Luz, P. E. Bolán, T. Maboni, M. R. Cosetin, M. F. da Silva and R. N. do Prado, "An Integrated Insulated Buck-Boost-Flyback Converter to Feed LED's Lamps to Street Lighting with Reduced Capacitances," *11th IEEE/IAS International Conference on Industry Applications (INDUSCON)*, 2014, pp. 1-6.

[21] G. Z. Abdelmessih and J. M. Alonso, "A new active Hybrid-Series-Parallel PWM dimming scheme for off-line integrated LED drivers with high efficiency and fast dynamics," *2016 IEEE Industry Applications Society Annual Meeting*, Portland, OR, 2016, pp. 1-8.

[22] Q. Luo, J. Huang, Q. He, K. Ma and L. Zhou, "Analysis and Design of a Single-Stage Isolated AC–DC LED Driver With a Voltage Doubler Rectifier," in *IEEE Transactions on Industrial Electronics*, vol. 64, no. 7, pp. 5807-5817, July 2017.

[23] J. Lam, N. El-Taweel and M. Abbasi, "An Output-Current-Dependent DC-Link Energy Regulation Scheme for a Family of Soft-Switched AC/DC Offline LED Drivers Without Electrolytic Capacitors," in *IEEE Transactions on Industrial Electronics*, vol. 64, no. 7, pp. 5838-5850, July 2017.

[24] U. Ramanjaneya Reddy and B. L. Narasimharaju, "Single-stage electrolytic capacitor less non-inverting buck-boost PFC based AC–DC ripple free LED driver," in *IET Power Electronics*, vol. 10, no. 1, pp. 38-46, 1 20 2017.

[25] M. F. Menke, R. V. Tambara, F. E. Bisogno, M. F. da Silva and Á. R. Seidel, "Universal input voltage LED driver with dimming capability and reduced DC-link capacitance," *IECON 2016 - 42nd Annual Conference of the IEEE Industrial Electronics Society*, Florence, 2016, pp. 3629-3634.

[26] Y. Wang, J. Huang, W. Wang and D. Xu, "A Single-Stage Single-Switch LED Driver Based on Class-E Converter," in *IEEE Transactions on Industry Applications*, vol. 52, no. 3, pp. 2618-2626, May-June 2016. doi: 10.1109/TIA.2016.2519324.

[27] J. Baek; S. Y. Chae, "Single-Stage Buck-Derived LED Driver With Improved Efficiency and Power Factor Using Current Path Control Switches," in IEEE Transactions on Industrial Electronics , vol.PP, no.99, pp.1-1

[28] M. G. Kim, "High-Performance Current-Mode-Controller Design of Buck LED Driver with Slope Compensation," in IEEE Transactions on Power Electronics , vol.PP, no.99, pp.1-1

[29] B. M. Lim, Y. H. Ko, Y. S. Jang, O. H. Kwon, S. K. Han and S. G. Lee, "A 200-V 98.16%-Efficiency Buck LED Driver Using Integrated Current Control to Improve Current Accuracy for Large-Scale Single-String LED Backlighting Applications," in *IEEE Transactions on Power Electronics*, vol. 31, no. 9, pp. 6416-6427, Sept. 2016.

[30] P. Y. Lin, T. J. Liang, C. W. Chang, K. H. Chen and B. K. Huang, "Buck-type wide-range dimmable LED driver," *2017 IEEE Applied Power Electronics Conference and Exposition (APEC)*, Tampa, FL, 2017, pp. 1563-1569.

[31] H. C. Kim, M. C. Choi, S. Kim and D. K. Jeong, "An AC–DC LED Driver With a Two-Parallel Inverted Buck Topology for Reducing the Light Flicker in Lighting Applications to Low-Risk Levels," in *IEEE Transactions on Power Electronics*, vol. 32, no. 5, pp. 3879-3891, May 2017.

[32] M. F. da Silva, J. Fraytag, M. E. Schlittler, T. B. Marchesan, M. A. Dalla Costa, J. M. Alonso and R. N. do Prado, "Analysis and Design of a Single-Stage High-Power-Factor Dimmable Electronic Ballast for Electrodeless Fluorescent Lamp," in *IEEE Transactions on Industrial Electronics*, vol. 60, no. 8, pp. 3081-3091, Aug. 2013.

[33] R. A. Pinto, J. G. Roncalio and R. N. do Prado, "Street lighting system using light emitting diode (LEDs) supplied by the mains and by batteries". *International Conference on New Concepts in Smart Cities: Fostering Public and Private Alliances (SmartMILE)*, pp. 1-7, Dec. 2013.

[34] J. Chen, R. Erickson and D. Maksimovic, "Averaged switch modeling of boundary conduction mode DC-to-DC converters." *Industrial Electronics Society, 2001. IECON '01. The 27th Annual Conference of the IEEE*, vol. 2, pp. 844-849, Nov-Dec. 2001.

[35] P. S. Almeida, D. Camponogara, M. Dalla Costa, H. Braga and J. M. Alonso, "Matching LED and Driver Life Spans: A Review of Different Techniques," in *IEEE Industrial Electronics Magazine*, vol. 9, no. 2, pp. 36-47, June 2015.

[36] A. Agrawal, K. C. Jana and A. Shrivastava, "A review of different DC/DC converters for power quality improvement in LED lighting load," *2015 International Conference on Energy Economics and Environment (ICEEE)*, Noida, 2015, pp. 1-6.

[37] B. Poorali and E. Adib, "Analysis of the Integrated SEPIC-Flyback Converter as a Single-Stage Single-Switch Power-Factor-Correction LED Driver," in *IEEE Transactions on Industrial Electronics*, vol. 63, no. 6, pp. 3562-3570, June 2016.

[38] A. Jha and B. Singh, "Bridgeless buck-boost PFC converter for multistring LED driver," *2017 IEEE Industry Applications Society Annual Meeting*, Cincinnati, OH, 2017, pp. 1-8.

[39] J. M. Alonso, J. Vina, D. G. Vaquero, G. Martinez and R. Osorio, "Analysis and Design of the Integrated Double Buck–Boost Converter as a High-Power-Factor Driver for Power-LED Lamps," in *IEEE Transactions on Industrial Electronics*, vol. 59, no. 4, pp. 1689-1697, April 2012.

[40] J. M. Alonso, A. J. Calleja, D. Gacio, J. Cardesín and E. López, "A long-life high-power-factor HPS-lamp LED retrofit converter based on the integrated buck-boost buck topology," *IECON 2011 - 37th Annual Conference of the IEEE Industrial Electronics Society*, Melbourne, VIC, 2011, pp. 2860-2865.